



Enhanced oral delivery of epigallocatechin gallate via expanding gastro-retentive films composed of chitosan and konjac glucomannan blends

Arnas Lakhiew¹, Rachanida Preparatana², Yaowaporn Sangsen³, Ruedeekorn Wiwattanapatapee^{1*} 

¹Faculty of Pharmaceutical Sciences, Prince of Songkla University, Hat Yai, Thailand.

²Faculty of Medical Technology, Prince of Songkla University, Hat Yai, Thailand.

³Faculty of Public Health and Allied Health Sciences, Sirindhorn College of Public Health Trang, Trang, Thailand.

ARTICLE HISTORY

Received on: 10/08/2025

Accepted on: 12/11/2025

Available Online: 05/12/2025

Key words:

Epigallocatechin gallate, expandable film, chitosan, konjac glucomannan, gastroretentive drug delivery systems, anti-obesity.

ABSTRACT

Epigallocatechin gallate (EGCG), a bioactive compound extracted from green tea, is known for its antioxidant, anti-inflammatory, and anti-obesity effects. However, it is prone to degradation in the gastrointestinal tract due to the alkaline pH and enzymatic activity in the intestine, leading to reduced therapeutic efficacy. To overcome this limitation, EGCG was incorporated into a chitosan-based expandable film designed for prolonged gastric retention and controlled release. Chitosan, a highly swelling polymer, was combined with konjac glucomannan (KGM) as a secondary polymer, along with sodium alginate and glycerin. This system exhibited significant swelling in simulated gastric fluid (pH 1.2), maintaining its expanded structure and achieving a sustained release of over 80% within 8 hours. The inclusion of KGM enhanced the film's tensile strength, improving its mechanical properties. Bioactivity studies demonstrated that the EGCG-loaded film significantly inhibited inflammation by reducing nitric oxide production in RAW 264.7 macrophage cells. Additionally, it suppressed lipid accumulation on 3T3-L1 adipocytes, supporting its potential anti-obesity effects. These findings suggest that the chitosan–KGM-based expandable film offers an effective gastro-retentive system for EGCG delivery, ensuring prolonged release and enhanced therapeutic benefits.

1. INTRODUCTION

Green tea (*Camellia sinensis*) has long been consumed in China and is now globally recognized for its health benefits, largely due to its bioactive catechins, including epicatechin, gallic acid, gallic acid gallate (GAG), epigallocatechin gallate (EGCG)—the most biologically active compound [1–3]. Among the catechins, EGCG exhibits the most potent biological activities, including antioxidant, anti-inflammatory, anti-obesity, neuroprotective, and metal-chelating properties [2,4]. However, its poor gastrointestinal absorption

and low stability in the intestinal environment, where it is rapidly hydrolyzed by microflora, limit its bioavailability [5]. To address this, strategies such as enhancing gastric retention have been investigated to improve EGCG delivery and efficacy [6].

Several strategies have been developed for targeted drug delivery to specific sites to enhance and prolong the absorption of therapeutic compounds. Gastro-retentive drug delivery systems are particularly effective for drugs with low stability at high alkaline pH and a narrow absorption window in the gastrointestinal tract [7]. These systems employ various mechanisms, including high-density systems, raft-forming systems, magnetic systems, superporous hydrogels, and expandable systems [7,8]. The common purpose of these approaches is to extend the release time of the drug to enhance absorption and bioavailability. Expandable systems, initially developed for veterinary use, offer an alternative method for

*Corresponding Author
Ruedeekorn Wiwattanapatapee, Faculty of Pharmaceutical Sciences,
Prince of Songkla University, Hat Yai, Thailand.
E-mail: ruedeekorn.w@psu.ac.th

drug delivery by prolonging gastric retention while facilitating oral administration. Among these devices, expandable films have been specifically engineered to increase in volume or alter their shape by swelling or unfolding upon contact with gastric fluids. Expansion occurs via osmosis (swelling) or mechanical shape memory (unfolding) when in contact with gastric fluid [9]. The expanded form resists gastrointestinal movement and prevents passage through the pyloric sphincter [10]. The water absorption properties of the polymer influence the expansion, ensuring that the swollen system's dimensions exceed those of the pyloric sphincter, thereby extending drug release [8]. Recently, polysaccharide-based expandable films have gained significant interest as gastroretentive carriers, owing to their biocompatibility, biodegradability, and capacity to undergo controlled swelling or dimensional increases upon contact with gastric fluids. Solvent casting has been identified as an effective, low-cost method for fabricating these polysaccharide-based expandable films.

Chitosan, a polysaccharide derived from chitin via alkaline deacetylation, is biodegradable, non-toxic, and biocompatible, making it attractive for biomedical use. Its mucoadhesive nature enhances drug absorption by prolonging gastrointestinal residence. Under acidic conditions, its amine groups enable gel formation and film casting, offering advantages over conventional materials [11]. Chitosan–sodium alginate (SA) combinations have been shown to regulate gelling strength and drug release rates [12], making them suitable for transdermal patches and wound dressings. Their biocompatibility, biodegradability, and ability to enhance structural stability also support their use in drug delivery systems such as hydrogels [13].

Konjac glucomannan (KGM), a polysaccharide extracted from *Amorphophallus konjac* tubers, is widely used in food manufacturing and film formation, particularly in packaging [14]. Composed of β -D-mannose and β -D-glucose linked by β -1,3- and β -1,4-glycosidic bonds [15], KGM is electrically neutral in water and exhibits high solubility, viscosity, adhesiveness, plasticity, and thickening ability. These properties make it a safe, non-toxic, biodegradable, and cost-effective material for food, pharmaceutical, and biomedical applications [16,17]. Unlike other natural polymers used for their gel-forming and swelling properties in gastrointestinal retention (e.g., alginate, chitosan, and cellulose derivatives), KGM remains underexplored in oral drug delivery. However, its film-forming and swelling capacity under acidic gastric conditions suggests strong potential for gastroretentive systems, particularly expandable films with sustained mechanical stability.

Starch, a biodegradable and hydrophilic polysaccharide, is widely used in food and pharmaceutical applications due to its availability and low cost [18]. Composed of amylose and amylopectin, its film properties depend on their ratio [19]. Cellulose, found in plant and marine cell walls, offers strong mechanical, chemical, and thermal stability [20]. Its hydroxyl groups enable hydrogen bonding, enhancing performance. Derivatives, such as hydroxypropyl methyl cellulose (HPMC), carboxymethyl cellulose (CMC), or hydroxyethyl cellulose (HEC), are commonly used as

film-forming agents in pharmaceuticals, cosmetics, and smart materials [21].

The rationale for this study lies in addressing the limited bioavailability of EGCG due to its poor gastrointestinal absorption and instability in the intestinal environment. To overcome these challenges, the research aims to develop a novel expandable gastroretentive dosage form using hydrophilic polymer-based composite films. By combining chitosan with additional film-forming agents such as KGM, starch, and cellulose derivatives, the study seeks to enhance the controlled release and gastric retention of EGCG. The properties of these films, including physical, chemical, and mechanical characteristics, were compared to identify formulations capable of improving the compound's biological efficacy.

2. MATERIALS AND METHODS

2.1. Materials

EGCG powder (98%) was purchased from Xi'an Nate Biological Technology (China). KGM Extract Powder was sourced from Asia Bioplex (Chonburi, Thailand). White chitosan (degree of deacetylation 85%, molecular weight 500,000) was obtained from BIO21 (Samutsakhon, Thailand). SA was sourced from Loba Chemie (Mumbai, India), Glycerin was acquired from P.C. Drug Center Co., Ltd. (Bangkok, Thailand), Glutinous rice starch (*Oryza sativa var. glutinosa*; 0.56% amylose content), and rice starch (*O. sativa*; 33.8% amylose content) were purchased from Cho Heng Rice Vermicelli Factory Co., Ltd. (Nakhon Pathom, Thailand), and mung-bean starch (*Vigna radiata*; 30%–45% amylose content) was obtained from Sitthinan Co., Ltd. (Bangkok, Thailand). Methocel K4MCR Premium was sourced from Rama Production Co., Ltd. (Bangkok, Thailand), while HEC and methyl cellulose (4,000 CPS) were purchased from Krungthepchemi Co., Ltd. (Bangkok, Thailand), and Loba Chemie (Mumbai, India), respectively. Hard gelatin capsules (size 00) were acquired from Capsugel (Bangkok, Thailand). RAW264.7 cells (murine macrophage cell line) and 3T3-L1 cells (murine preadipocyte cell line) were obtained from the American Type Culture Collection, ATCC (VA, USA). Lipopolysaccharide (LPS, from *Escherichia coli*) and indomethacin were purchased from Sigma Aldrich (Sigma Aldrich, MO, USA). Fetal calf serum (FCS), Roswell Park Memorial Institute 1640 medium (RPMI-1640), Dulbecco's modified Eagle's medium (DMEM), Phosphate buffer saline (PBS), and Penicillin-streptomycin were supplied by Gibco (Invitrogen, CA, USA). The 96-well microplates were sourced from Nunc (Roskilde, Denmark), and dimethyl sulfoxide (DMSO) was from Amresco (OH, USA). All other chemicals were analytical or pharmaceutical grades.

2.2. Preparation of expandable film containing EGCG

The composites of all prepared formulations are presented in Table 1. Chitosan was used as a primary film-forming agent, with secondary film-forming agents including KGM, starch (glutinous rice, rice, and mung-bean starch), and cellulose derivatives (HPMC E4M, HEC, MC 4000). Chitosan was dissolved in 45 g of 1 M acetic acid, while each secondary film-forming agent was separately dissolved in 45 g of deionized

Table 1. Formulations of expandable films composed of chitosan and secondary film-forming agents.

Formulation	EGCG (g)	Chitosan (%)	Glycerin (%)	SA (%)	KGM (%)	Glutinous Rice starch (%)	Rice starch (%)	Mung bean starch (%)	HPMC K4M (%)	Methyl cellulose 4000 (%)	HEC (%)
Chitosan	2.1	1.5	2	0.1	-	-	-	-	-	-	-
A1	2.1	1.5	2	0.1	0.5	-	-	-	-	-	-
A2	2.1	1.5	2	0.1	1.0	-	-	-	-	-	-
A3	2.1	1.5	2	0.1	1.5	-	-	-	-	-	-
B1	2.1	1.5	2	0.1	-	0.5	-	-	-	-	-
B2	2.1	1.5	2	0.1	-	1.0	-	-	-	-	-
B3	2.1	1.5	2	0.1	-	1.5	-	-	-	-	-
B4	2.1	1.5	2	0.1	-	-	0.5	-	-	-	-
B5	2.1	1.5	2	0.1	-	-	1.0	-	-	-	-
B6	2.1	1.5	2	0.1	-	-	1.5	-	-	-	-
B7	2.1	1.5	2	0.1	-	-	-	0.5	-	-	-
B8	2.1	1.5	2	0.1	-	-	-	1.0	-	-	-
B9	2.1	1.5	2	0.1	-	-	-	1.5	-	-	-
C1	2.1	1.5	2	0.1	-	-	-	-	0.5	-	-
C2	2.1	1.5	2	0.1	-	-	-	-	1.0	-	-
C3	2.1	1.5	2	0.1	-	-	-	-	1.5	-	-
C4	2.1	1.5	2	0.1	-	-	-	-	-	0.5	-
C5	2.1	1.5	2	0.1	-	-	-	-	-	1.0	-
C6	2.1	1.5	2	0.1	-	-	-	-	-	1.5	-
C7	2.1	1.5	2	0.1	-	-	-	-	-	-	0.5
C8	2.1	1.5	2	0.1	-	-	-	-	-	-	1.0
C9	2.1	1.5	2	0.1	-	-	-	-	-	-	1.5

water at varying concentrations and stirred overnight until completely dissolved. For the starch solution, an additional step involved heating the mixture at 100°C for 1 hour to form a gel layer, followed by overnight stirring. Glycerin and SA were then added to the solution. The required amount of EGCG was incorporated to obtain 100 mg per individual film piece (40 × 20 mm), the total solution weight was adjusted to 100 g with deionized water, and the mixture was homogenized for 5 minutes to obtain a homogenous solution, which was degassed using a sonicator until the bubbles disappeared. The resulting solution (50 g) was poured into a glass petri dish (78 cm² area) and dried for 48 hours at 45°C. The composite films were peeled, cut into rectangle pieces (40 × 20 mm), folded in a zigzag manner, and then loaded into hard gelatin capsule (size 00).

2.3. Physicochemical characterization of EGCG-loaded expandable films

2.3.1. Film weight and thickness

Each film formulation was prepared in a rectangular shape (40 × 20 mm). Ten samples were weighed using an analytical balance (XB 220 A, Precisa, Dietikon, Switzerland). The thickness of samples was measured at multiple locations using a digital vernier caliper (V6-154, Kovet, Bangkok, Thailand). The average weight, thickness, and SD values were calculated and reported ($n = 10$).

2.3.2. Tensile strength measurement of films

Tensile strength of the films was measured using a texture analyzer (TA.XT plus Texture Analyzer, Micro Systems, Surrey, UK). Film strips were cut into rectangular shapes and held between two clamps positioned 10 mm apart. To prevent film breakage, a plastic card was attached to the grooves of the clamps, covering the surface of film. The samples were longitudinally stretched at a rate of 2.0 mm/sec until rupture, and the applied force at the breaking point was recorded. Tensile strength measurements were obtained for each formulation ($n = 5$), and the tensile strength was calculated using Equation 1.

$$\text{Tensile strength (MPa)} = \frac{\text{Force at break (N)}}{\text{Initial cross section of the sample (mm}^2\text{)}} \quad (1)$$

2.3.3. Film unfolding behavior and film expansion

Film samples (40 × 20 mm) were individually placed into size 00 hard gelatin capsules, folded in a zigzag manner before filling. Dissolution testing was examined using a dissolution tester (Electrolab, Mumbai, India) with simulated gastric fluid (SGF, 0.1 N hydrochloric acid, pH 1.2, 900 m;) at 37°C ± 0.5°C. The samples were placed in a USP 30 rotating basket dissolution apparatus and tested at a rotation speed of 100 rpm. Observation was made at time intervals of 5, 10, 15,

30, 60, 120, 240, and 480 minutes. The swollen films at 480 minutes, exhibiting a rectangular shape, were measured for length and width to calculate the fold change of film expansion in surface area ($n = 3$).

2.3.4. Film swelling behavior

The increased weight of the film was measured using an analytical balance (XB 220 A, Precisa, Dietikon, Switzerland). Dissolution testing was conducted in a dissolution tester (Electrolab, Mumbai, India) with SGF (0.1 N hydrochloric acid, pH 1.2, 200 ml) at $37 \pm 0.5^\circ\text{C}$, at a rotation speed of 100 rpm. The weight of samples was recorded before (W1) and after dissolution (W2) at time intervals of 5, 10, 15, 30, 60, 120, 240, and 480 minutes. Fluid absorption and weight increase were calculated using Equation 2 and reported as mean \pm SD ($n = 3$).

$$\text{Fluid absorption} = \frac{(W2 - W1)}{W1} \times 100 \quad (2)$$

2.3.5. EGCG release profiles from expandable films

The drug release profile of the film formulations was determined using a USP 30 rotating basket dissolution apparatus at a rotating speed of 100 rpm in SGF at pH 1.2 (0.1 N hydrochloric acid, 900 ml) at $37^\circ\text{C} \pm 0.5^\circ\text{C}$. Samples (10 ml) were withdrawn at 5, 10, 15, 30, 60, 120, 240, and 480 minutes with fresh medium replaced after each withdrawal. The samples were filtered and analyzed using the UV-Vis spectroscopy. The cumulative percentage of drug release was calculated, and data are presented as mean \pm SD. The experiments were repeated three times of each formulation.

To study and compare the effect of pH on EGCG release, the three chitosan film formulations combined with different types of polysaccharide—KGM, starch, and cellulose derivatives—were selected based on their suitable drug release profiles in SGF pH 1.2; the same samples were then determined in acetate buffer pH 4.5 under identical conditions.

2.3.6. Release kinetics of EGCG

The kinetics of EGCG release from expandable films were investigated by plotting the release data obtained in pH 1.2 medium to fit several mathematical models of drug release, including zero-order [22], first-order [23], Hixson–Crowell [24], Higuchi [25], and Korsmeyer–Peppas model [26].

2.3.7. Determination of EGCG content

The EGCG-loaded expandable films ($1 \times 1 \text{ cm}^2$) were accurately weighed and cut into small pieces, and then placed in a 250 ml Erlenmeyer flask with 100 ml of deionized water. The samples were sonicated for 6 hours, followed by shaking at 40°C for 24 hours using a Benchtop Orbital Shaker (NJ, USA) to extract and completely dissolve the EGCG from the film. The Filtrate was collected after filtration through a $0.45 \mu\text{m}$ nylon filter. The samples were quantitatively analyzed using UV-Vis spectrophotometry at a wavelength of 274 nm ($n = 5$).

2.3.8. Morphology of the selected expandable film

The morphology of the expandable films was determined by scanning electron microscopy (SEM, Quanta

400, FEI, USA). The film formulation of chitosan with glucomannan (A2) was coated with gold before examination at an accelerating voltage of 20 keV.

2.3.9. Fourier transform infrared studies

Fourier transform infrared (FTIR) spectroscopy was performed using a PerkinElmer 400 instrument. KBr and the samples were compressed to prepare pellets for scanning over the range $450\text{--}4,000 \text{ cm}^{-1}$ to identify the functional groups present in excipients of the expandable films.

2.3.10. X-ray diffraction studies

X-ray powder diffraction was performed by using an X-ray diffractometer. The diffraction pattern was analyzed at 2θ from 2° to 50° , with an angular variation of $0.02^\circ/\text{sec}$, while applying 40 kV and a wavelength of 0.3 \AA .

2.3.11. Differential scanning calorimetry studies

Differential scanning calorimetry (DSC) was conducted using a DSC3 calorimeter (Mettler Toledo, Inc., Columbus, OH). Approximately 5 mg of the sample was weighed and heated from 20°C to 300°C at a rate of 5°C per minute. For each thermogram, the onset melting temperature, and peak temperature, related to enthalpy, were recorded.

2.4. Evaluation of biological activities

2.4.1. Determination of antioxidant activity

A methanolic solution of 0.1 mM 2,2-diphenyl-1-picrylhydrazyl (DPPH) was prepared by diluting the DPPH reagent in 99.9% methanol, followed by incubation in the dark at room temperature [27]. A $100 \mu\text{l}$ aliquot of this solution was transferred to 96-well plates and combined with $300 \mu\text{l}$ of EGCG formulations at concentrations of 100, 50, 25, 12.5, 6.25, and $3.13 \mu\text{g/ml}$. For comparison, solutions of ascorbic acid (reference compound) and blank samples were prepared at the same six concentrations using the same procedure. The mixtures were incubated in the dark for 30 minutes, followed by absorbance measurement using UV spectroscopy. The absorbance of each mixture in the 96-well plates was recorded at 517 nm with a microplate reader. The experiment was performed in triplicate, and free radical scavenging activity was calculated using Equation 3 ($n = 3$).

$$\text{Radical scavenging activity (\%)} = \left[1 - \left(\frac{B}{A} \right) \right] \times 100 \quad (3)$$

Where A represents the absorbance of methanol without sample (control), and B represents the absorbance of the sample.

2.4.2. In vitro cytotoxic and anti-inflammatory activity

2.4.2.1. In vitro cytotoxicity test on macrophage cells

Cytotoxic activity was assessed in RAW264.7 macrophages. The cells were prepared and seeded at a density of 80,000 cells/well in a 96-well plate and incubated for 12–16 hours. Various concentrations of EGCG formulations, EGCG

standard, blank, and the positive control indomethacin (100, 50, 25, 12.5, 6.25, and 3.13 µg/ml) were then treated to the cultured cells, followed by a 24-hour incubation. Afterward, methyl tetrazolium (MTT) solution (5 mg/ml in PBS) was diluted in medium (1:20), and 100 µl was added to each well containing RAW264.7 cells. The cells were incubated for 2 hours, after which the supernatant was removed, and 200 µl of DMSO was added to dissolve the formazan crystals. Absorbance was measured at 570 nm using a microplate reader (Biotek model PowerWave X, Santa Clara, CA). Cell viability was calculated and expressed as a percentage of cell viability according to Equation 4 ($n = 3$). Furthermore, IC_{50} values were determined as the concentration of the sample required to inhibit cell proliferation by 50%.

$$\text{Cell viability (\%)} = \left[\frac{A_{\text{sample}}}{A_{\text{control}}} \right] \times 100 \quad (4)$$

Where A_{sample} and A_{control} represent the absorbance at 570 nm of the test sample and control, respectively.

2.4.2.2. Anti-inflammatory activity assay

Anti-inflammatory activity was assessed by measuring the inhibition of nitric oxide (NO) production in RAW264.7 cells. The cells were cultured in RPMI 1640 medium supplemented with 0.1% sodium bicarbonate, 2 mM L-glutamine, 100 units/ml penicillin G, 100 µg/ml streptomycin, and 10% fetal bovine serum (FBS). Cells were seeded at a density of 80,000 cells/well in a 96-well plate and incubated at 37°C under a 5% CO₂ atmosphere for 12–16 hours. Various concentrations of the samples, as used in the cytotoxicity test, were then treated to cells exposed to LPS to induce inflammation, followed by a 24-hour incubation [28]. NO production was quantified by measuring nitrite levels in the culture medium using the Griess reagent. Cells not exposed to LPS or EGCG-containing samples were used as a negative control. Optical density was measured at 570 nm using a microplate reader (Biotek model PowerWave X, Santa Clara, CA), with indomethacin as the positive control ($n = 3$).

2.4.3. In vitro cytotoxic and anti-obesity activity

2.4.3.1. Cell culture

The 3T3-L1 cell lines are grown in 75 cm² plastic cell culture flasks maintained in DMEM (Gibco) supplemented with 10% FBS and 1% antibiotics (100 mg/ml streptomycin and 100 U/ml penicillin, Gibco). The cells are incubated in a 95% CO₂ at 37°C. Culture media is changed every 3 days; after 80% confluence, the cells were trypsinized by using trypsin-EDTA solution for culture cells at 37°C. Cell suspensions are prepared at optimized density before evaluating anti-obesity effect.

2.4.3.2. In vitro cytotoxicity test on adipose cells

The preadipocyte of 3T3-L1 cells was cultured in 96-well plates with a density of 5,000 cell/well, and cultured in differentiation medium, DMEM with high glucose, supplemented with 10% FCS and 1% penicillin-streptomycin.

Upon full differentiation, the cells were treated with various concentrations of EGCG standard powder, EGCG-containing samples, or blank formulation for 24 hours. Then, the MTT assay was performed as described in the cytotoxicity test for macrophage cells. Cell viability was calculated as a percentage of control using Equation 4 ($n = 3$).

2.4.3.3. Determination of inhibitory activity on adipocyte differentiation

The anti-obesity activity is evaluated by using 3T3-L1 preadipocyte cells. Briefly, 3T3-L1 preadipocytes were seeded on 48-well plates (1.5×10^4 cells/well) and cultured in differentiation medium. Once the cells reached confluence (after 5 days), the undifferentiated group (negative control) was maintained in the same culture medium. In contrast, the differentiation groups—including the differentiated or positive control, blank, EGCG standard, and samples at 2, 10, and 50 µg/ml—were induced using differentiation medium supplement with 0.5 mM isobutyl methylxanthine (IBMX), 1 µM dexamethasone, and 10 µM/ml bovine insulin (induction medium). After 2 days, the induction medium was replaced with differentiation medium, which was refreshed every 2 days thereafter. The experiment was conducted for at least 8 days post-induction.

The inhibition activity of lipid droplets in the cells was assessed by Oil Red O staining, which strongly stains lipids. The cells were washed with PBS, fixed with 10% formaldehyde in PBS for 15 minutes at room temperature, and then incubated with a dye solution diluted in 40% 2-propanol for 100 minutes at room temperature. The elute (100 µl) was transferred to a 96-well microtiter plate, and cells not exposed to EGCG-containing samples served as the negative control. Absorption was measured at 570 nm using a microplate reader, using EGCG as a positive control to compare the activity of the samples ($n = 3$).

2.5. Statistical analysis

The data are expressed as the mean \pm SD. Data analysis was performed by Student's *t*-test and one-way analysis of variance. Statistical probability (*p* values) of <0.05 was considered statistically significant.

3. RESULTS AND DISCUSSION

3.1. Physicochemical characterization of EGCG-loaded expandable films

3.1.1. Film weight and thickness

As shown in Table 2, the weight of films containing EGCG ranged from 395.2 ± 0.02 to 554.3 ± 0.02 mg, depending on the polymer type and concentration. The results of formulations A1–A3, which incorporated increasing concentrations of glucomannan, showed the highest weights, followed by formulations B1–B9 which varied in starch types and concentrations, and formulations C1–C6 which included different cellulose derivatives. The high molecular weight of glucomannan contributed to its high density, thus increasing the film weight. Film thickness ranged from 0.45 ± 0.02 to 0.54

± 0.01 mm, with low SDs, indicating good reproductivity and dose uniformity of the preparation method.

3.1.2. Tensile strength of films

The tensile strength of the films reflects their ability to resist the mechanical movement in the stomach, demonstrating their gastro-retentive properties. Pure chitosan films (1.5%), used as the control, exhibited a tensile strength of 8.29 ± 0.50 MPa. The incorporation of additional polymers into the film matrix resulted in alteration of mechanical strength. All formulations contained 1.5 % of chitosan as the primary polymer, combined with a secondary polymer. As shown in Table 2, films containing glucomannan as a secondary polymer showed the highest tensile strength, with the strength increasing proportionally to glucomannan content (0.5%, 1.0%, and 1.5%). This improvement is attributed to the synergistic interaction between chitosan and glucomannan, the latter contributing elasticity to the composite structure. According to Chen *et al.* [29], glucomannan-based films exhibit improved mechanical properties due to a stable microstructure.

Films containing 0.5 % starches (glutinous rice, rice, and mung bean) exhibited tensile strengths of 4.43 ± 0.61 MPa (B1), 2.67 ± 0.40 MPa (B4), and 2.03 ± 0.33 MPa (B7), respectively. Among these, glutinous rice starch showed the highest tensile strength, owing to its higher amylopectin-to-

amylose ratio, which influences the gelatinization properties [30]. The branched structure of amylopectin reduces retrogradation, whereas non-glutinous rice starch is more prone to retrogradation, resulting in lower tensile strength. Retrogradation occurs when high-amylose glucose molecules reassociate after gelation, increasing stiffness and reducing flexibility. Xu *et al.* [31] found that increasing starch content in chitosan film increases tensile strength up to the maximum point, after which further starch addition leads to a decline in strength [32].

Films containing 0.5% cellulose derivatives (HPMC [C1], MC [C4], and HEC [C7]) combined with 1.5% chitosan exhibited higher tensile strengths compared to starch-based films. The excellent film-forming ability of hydrophilic cellulose derivatives contributes to their elasticity and structural strength. The strength of HPMC and cellulose films is enhanced by intermolecular hydrogen bonding between the OH groups of HPMC and the functional groups of the other polymers [33]. Zanchetta *et al.* [34] reported that small amounts of chitosan in copolymer films improve both tensile strength and plasticity, similar to the effect observed with HPMC.

3.1.3. Film unfolding behavior

Film samples were folded in a zigzag manner and inserted into hard gelatin capsules. Upon capsule dissolution in

Table 2. Characterization of EGCG-loaded expandable films in terms of weight, thickness, tensile strength, and film expansion.

Formulation	Weight (mg)	Thickness (mm)	Tensile strength (MPa)**	Film expansion (Area increased, fold)*
Chitosan	377.1 ± 0.01	0.42 ± 0.01	8.29 ± 0.50	3.31 ± 0.19
A1	499.2 ± 0.01	0.52 ± 0.03	10.03 ± 1.30 ^a	4.58 ± 0.23 ^a
A2	536.7 ± 0.02	0.53 ± 0.02	11.79 ± 1.11 ^a	4.69 ± 0.12 ^a
A3	554.3 ± 0.02	0.54 ± 0.01	12.62 ± 0.98 ^b	5.04 ± 0.12 ^a
B1	439.0 ± 0.01	0.47 ± 0.03	4.43 ± 0.61 ^c	3.63 ± 0.11 ^b
B2	474.7 ± 0.01	0.50 ± 0.02	5.08 ± 0.41 ^d	4.10 ± 0.10 ^b
B3	489.0 ± 0.02	0.51 ± 0.01	6.33 ± 0.83 ^d	4.67 ± 0.20 ^a
B4	426.0 ± 0.01	0.46 ± 0.02	2.67 ± 0.40 ^e	3.22 ± 0.56 ^b
B5	467.4 ± 0.02	0.49 ± 0.03	2.76 ± 0.36 ^e	3.82 ± 0.31 ^b
B6	477.8 ± 0.01	0.51 ± 0.02	3.25 ± 0.57 ^e	4.12 ± 0.13 ^b
B7	425.0 ± 0.01	0.45 ± 0.01	2.03 ± 0.33 ^f	3.24 ± 0.10 ^b
B8	465.2 ± 0.01	0.48 ± 0.02	2.06 ± 0.47 ^f	3.90 ± 0.61 ^b
B9	469.9 ± 0.01	0.49 ± 0.02	2.12 ± 0.41 ^f	4.21 ± 0.30 ^a
C1	414.5 ± 0.01	0.45 ± 0.01	10.20 ± 0.68 ^b	4.13 ± 0.12 ^b
C2	456.1 ± 0.01	0.46 ± 0.02	10.41 ± 0.45 ^b	4.78 ± 0.11 ^a
C3	476.4 ± 0.02	0.47 ± 0.02	11.17 ± 0.79 ^b	4.93 ± 0.08 ^a
C4	395.2 ± 0.02	0.45 ± 0.01	11.84 ± 0.81 ^a	4.20 ± 0.10 ^a
C5	440.4 ± 0.01	0.46 ± 0.02	12.27 ± 0.97 ^a	4.62 ± 0.09 ^a
C6	458.9 ± 0.02	0.46 ± 0.01	12.67 ± 0.74 ^a	4.86 ± 0.20 ^a
C7	413.3 ± 0.02	0.45 ± 0.02	10.43 ± 0.77 ^b	4.05 ± 0.09 ^a
C8	455.5 ± 0.01	0.47 ± 0.01	10.90 ± 0.74 ^b	4.53 ± 0.25 ^a
C9	471.6 ± 0.01	0.47 ± 0.02	11.08 ± 0.68 ^b	4.71 ± 0.13 ^a

^aStatistically significant differences compared to pure chitosan films ($p < 0.05$); ^bcompared to A2 formulation ($p < 0.05$); ^ccompared to A3 formulation ($p < 0.05$); ^dcompared to B1 formulation ($p < 0.05$); ^ecompared to B3 formulation ($p < 0.05$); ^fcompared to B6 formulation ($p < 0.05$) ($n = 10$). Data are presented as mean ± SD; *($n = 3$) and **($n = 5$).

SGF, the films absorbed water, resulting in increased dimension and transformation into a rectangular shape. Complete unfolding occurred within 15–30 minutes, continuing to expand for up to 8 hours. The film's rolling pattern was attributed to its basket-like structure. Reversible shape memory polymers (RSMPs) can switch shapes in response to stimuli such as water. Chitosan/glycerin film can undergo these transformations, as hydrogen bonding between the amino and hydroxyl groups of chitosan changes, leading to protonation of the amino group and electrostatic interactions [35].

Films containing KGM (A2) and cellulose derivatives (C2, C5, and C8) maintained their strength with minimal erosion, indicating their ability to withstand mechanical forces in the stomach. In contrast, starch-based films (B2, B5, and B8) eroded in SGF, losing structural integrity and suggesting they might not sustain EGCG release in the stomach for 8 hours. The hydrophilicity of EGCG attracts water into the films, and while glucomannan absorbs large amounts of water to preserve film strength, starches absorb moisture through their hydroxyl groups, weakening mechanical strength [14].

All film formulations exhibited similar unfolding patterns, with film thickness increasing due to water absorption within 30 minutes. Films with high strength and elasticity maintained their integrity up to 8 hours. Formulation C2, although having greater thickness, preserved its structure and remained intact for 8 hours. Films made from glutinous rice starch and chitosan showed rapid swelling within an hour, reaching equilibrium after 2 hours. Films containing glucomannan (A2) and cellulose derivatives (C2) exhibited stronger performance than starch-based films, with less erosion, indicating greater film strength (Fig. 1). The starch-based films experienced erosion, which led to coagulation and loss of their original shape. The interaction between starch and chitosan reduced film solubility, contributing to this erosion [36]. In contrast, films containing glucomannan or cellulose derivatives absorbed more water and maintained their strength, preserving their original shape longer.

Glycerin, as a plasticizer, enhanced the flexibility of the films, contributing to their shape memory properties. Films with glycerin demonstrated greater elasticity and could revert from a zigzag shape more quickly than those without [9,35]. The incorporation of cellulose derivatives such as HPMC further improved elasticity, enabling the films to maintain their original shape and structure for up to 8 hours.

3.1.4. Film expansion (increased in area)

The results of the film expansion in terms of surface area are shown in Table 2. The film composed of chitosan combined with KGM exhibited the highest expansion, with a 5-fold increase in surface area compared to its original dimensions. This phenomenon can be attributed to significant aqueous absorption. Despite the expansion, the film maintained sufficient strength to preserve its structure without significant fragility or damage. The expansion ranking, based on the increase in surface area, is as follows: KGM > glutinous rice starch > cellulose derivatives. While films containing various starch types and chitosan (formulations B1–B9) exhibited high swelling ratios, starch-based formulations were more prone to

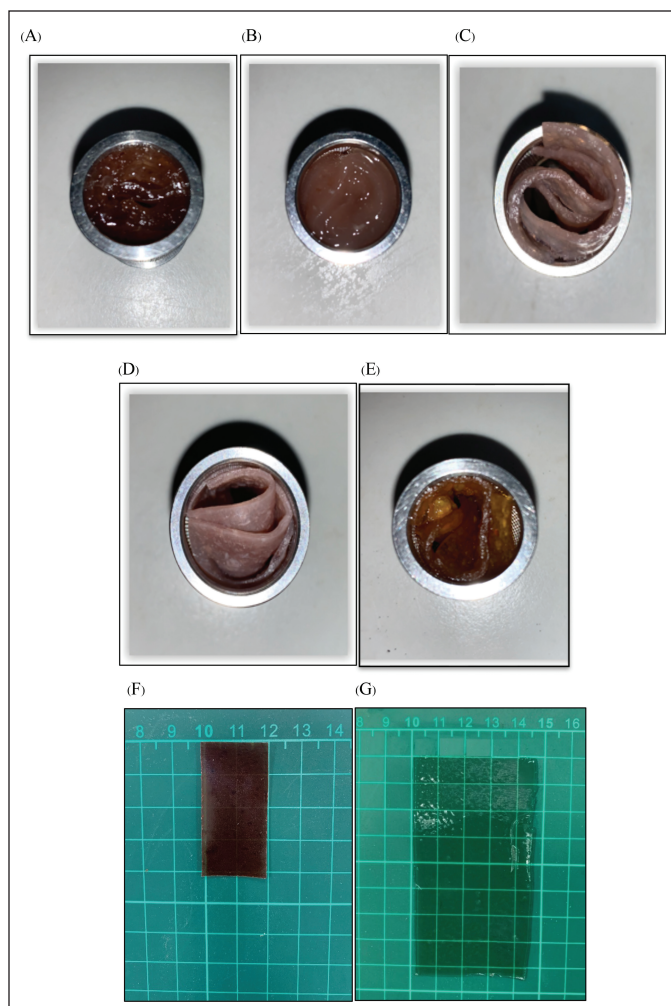


Figure 1. Characteristics of the swollen stage of expandable films composed of chitosan as the primary polymer combined with the secondary polymer: (A) Konjac glucomannan; (B) Glutinous rice starch; (C) HPMC K4M; (D) Methyl cellulose 4000; (E) HEC, and Film expansion of formulation A2 containing chitosan and konjac glucomannan: (F) Dried state; (G) Swollen state.

fragility and erosion compared to formulations A1–A3 and C1–C9. This observation is consistent with the lower mechanical strength of starch-containing formulations, as supported by previous studies showing that chitosan–glutinous rice starch films exhibit less dimensional expansion than those combined with KGM [37].

3.1.5. Swelling behavior (weight increased)

The swelling behavior of the films is shown in Figures 1 and 2. Films were immersed in SGF, and their weight was measured over time, revealing their aqueous absorption properties. Chitosan exhibited the highest swelling, significantly expanding the film (data not shown). However, its biodegradability and erosion limit its ability to withstand the mechanical force in the stomach. Combining chitosan with other polysaccharides, such as KGM, enhances film strength, allowing it to last for up to 8 hours in the stomach (Fig. 1).

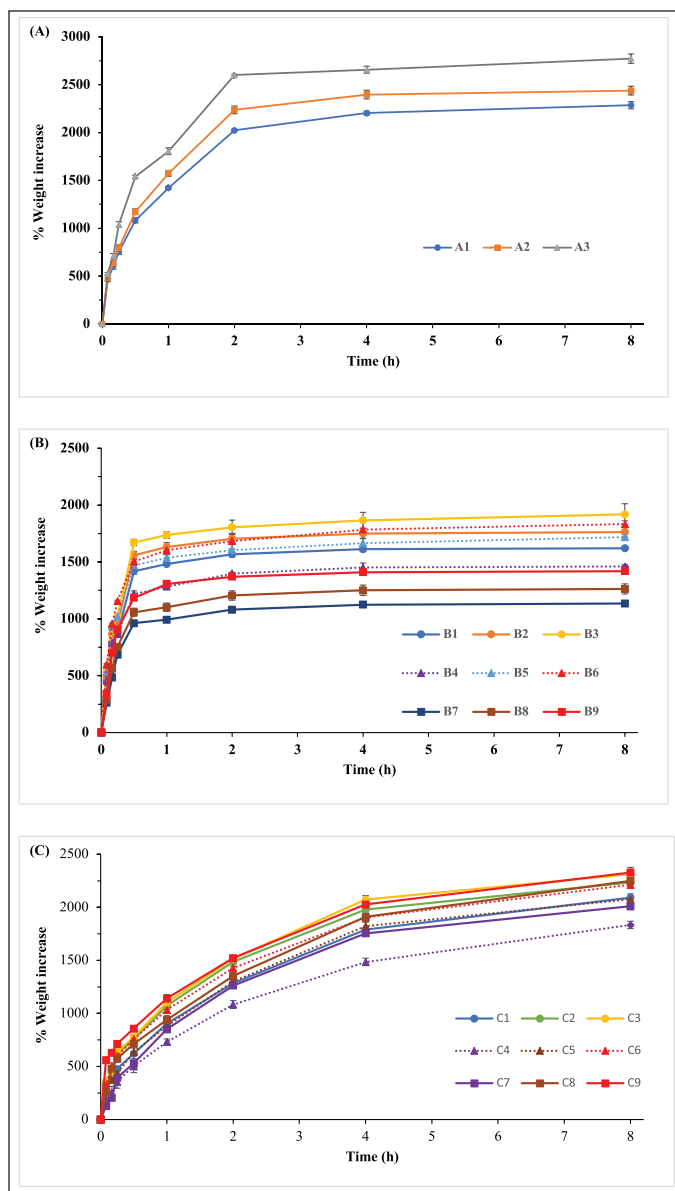


Figure 2. Swelling behavior (weight increased) of expandable films: (A) Chitosan combined with konjac glucomannan (A1–A3); (B) Chitosan combined with starches (B1–B9); (C) Chitosan combined with cellulose derivatives (C1–C9) ($n = 3$, mean \pm SD).

Formulation A3 (chitosan-KGM) showed the highest increase in weight ($2,772.8\% \pm 49.0\%$) after 2 hours, with weight remaining stable up to 8 hours. In comparison, starch-based formulations (B1–B9) exhibited swelling, though to a lesser extent than chitosan–KGM films. This may be attributed to variations in hydrogen bonding capacity; while starch, chitosan, and KGM contain hydrophilic groups ($-\text{OH}$, $-\text{NH}$), KGM possesses a higher density of functional groups, enabling stronger water interactions. Hydrophobic regions also contribute via secondary bound water. Total bound water increases until equilibrium swelling is reached, occupying pore spaces with both free and bound water [38]. The glutinous rice starch exhibited the highest swelling capacity ($1,918.7\% \pm 93.4\%$ for formulation

B3) due to its high amylopectin content. This is consistent with a previous report [32] that glutinous starch enhanced the swelling of chitosan films in gastric fluid (pH 1.2). At pH 1.2 and 4.5, higher chitosan content improved swelling due to its protonation below its pK_a (~ 6.5).

While cellulose derivatives combined with chitosan (C1–C9) showed a gradual increase in weight over an 8-hour period, HPMC formed a gel structure that reduced erosion and enhanced barrier properties. Compared to previous reports, expandable films composed of KGM and chitosan demonstrated greater area expansion and gastric volume occupancy than those made with xanthan gum, Carbopol 934P, and ethyl cellulose, which exhibited a low swelling index ($18.55\% \pm 0.14\%$ to $102.12\% \pm 0.12\%$) [39]. This is consistent with the report that HPMC-based films had high mechanical strength but limited swelling [11]. The enhanced swelling of chitosan-based films may result from water disrupting hydrogen bonds, leading to the formation of bound water and increased water absorption [35].

3.1.6. EGCG release profiles from expandable films

3.1.6.1. EGCG release profiles from the films in SGF pH 1.2

As shown in Figure 3A, expandable films composed of KGM and chitosan formed a thick structure upon exposure to SGF, likely due to the high molecular weight of the polymers. The films expanded in all dimensions and turned brown. The unfolding behavior and swelling capacity influenced the EGCG release profile, with KGM macromolecules enhancing gelation, viscosity, plasticity, and thickening properties. As a result, the formulation containing 1.5% chitosan and 1.0% KGM achieved 50% drug release at 4 hours and 90% at 8 hours. Furthermore, increasing KGM concentration reduced EGCG release, indicating a sustained release effect. Formulations A1 and A2, containing 0.5% and 1.0% KGM, respectively, released over 80% of EGCG within 8 hours. Few studies have explored drug release from chitosan–KGM blend films. Basak and Singhal [40] reported that KGM enhanced the structural resilience of composite hydrogels, enabling controlled *in vitro* release of riboflavin. Similarly, the combination of KGM with xanthan gum to fabricate films improved the diffusion coefficients of theophylline and diltiazem [41]. However, these systems formed viscous gels that hindered drug release. In contrast, formulation A2 (chitosan–KGM film) maintained structural integrity without forming a viscous gel over 8 hours, facilitating sustained drug release.

Formulations containing chitosan combined with varying starch types—glutinous rice starch (formulations B1–B3), rice starch (formulation B4–B6), and mung bean starch (formulation B7–B9)—showed that the lower starch content (1.0% of starch with 1.5% chitosan), achieved 80% drug release at 8 hour (Fig. 3B). Increased starch content (formulations B3, B6, and B9) acted as a barrier to EGCG release, with glutinous rice starch promoting the highest release due to its high amylopectin content, which enhanced swelling and facilitated diffusion and erosion mechanisms. In contrast, Kaewkroek *et al.* [30] reported that increased polymer content in chitosan–glutinous rice starch films reduced 6-gingerol release by

increasing film stiffness and tensile strength, thus limiting water penetration [30].

Films with cellulose derivatives combined with chitosan expanded upon contact with SGF and showed good

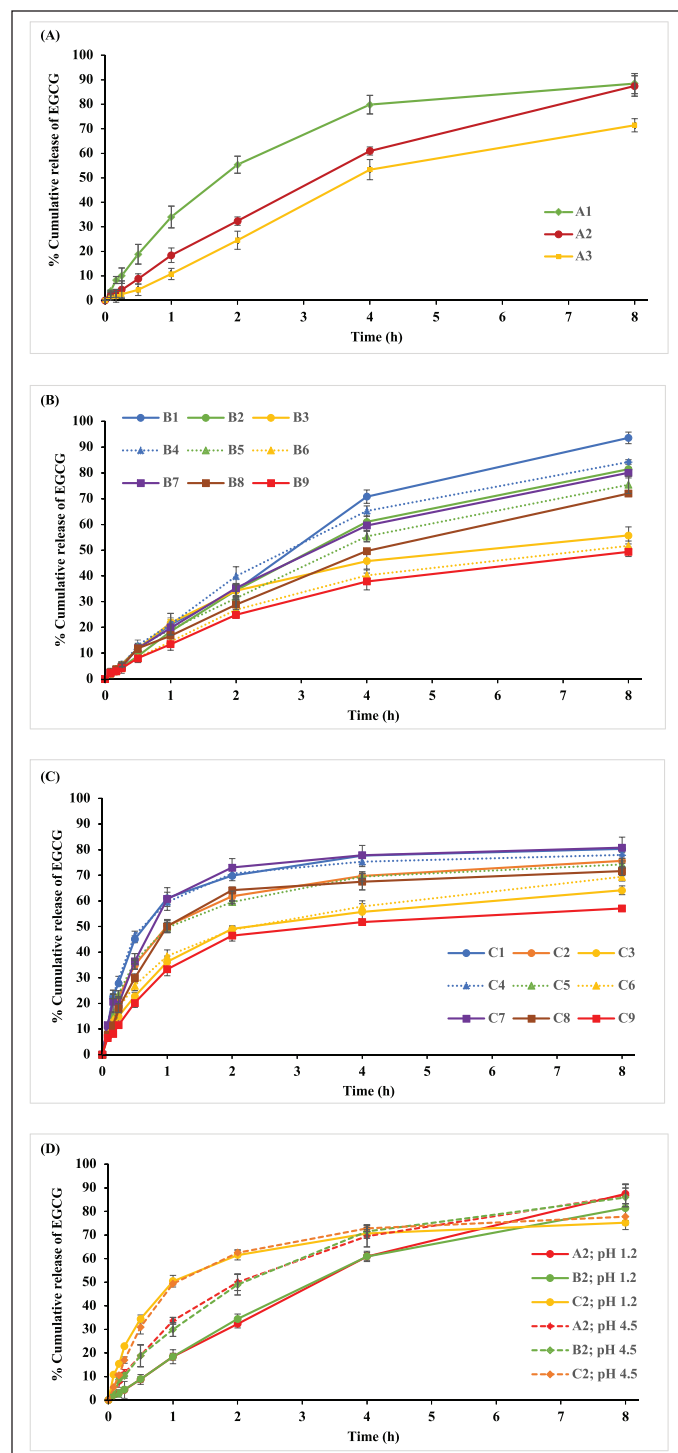


Figure 3. Drug release profile in SGF pH 1.2 of expandable films: (A) Chitosan combined with konjac glucomannan (A1–A3); (B) Chitosan combined with starches (B1–B9); (C) Chitosan combined with cellulose derivatives (C1–C9); and (D) Drug release profile of formulation A2, B2, and C2 in SGF pH 1.2 and in acetate buffer pH 4.5 ($n = 3$, mean \pm SD).

tensile strength. These films exhibited rapid EGCG release in the first 2 hours, likely due to the higher water solubility of cellulose derivatives (Fig. 3C). After 2 hours, the films maintained their strength, leading to the sustained release throughout 8 hours. However, the release of EGCG was lower (70%–80%) compared to other polysaccharide-based films, as the gel barrier formed by cellulose derivatives obstructed EGCG release through erosion, with diffusion being the dominant release mechanism. Therefore, formulation A2 (1% KGM), B2 (1% glutinous rice starch), and C2 (1% HPMC K4M) were selected for further testing due to their desirable expandable properties and good physicochemical, swelling, and drug release profiles.

3.1.6.2. EGCG release profiles from the films and their kinetics of release in pH 4.5

Formulation A2 was evaluated for its dissolution profile in an acetate buffer solution at pH 4.5 to compare EGCG release with pH 1.2, as shown in Figure 3D. The results showed higher EGCG release in the pH 4.5 solution during the first 4 hours. In acidic conditions (pH 1.2), chitosan exhibited more swelling due to its amino functional groups, forming a gelatinous layer that acted as a barrier, thus sustaining the release of EGCG and resulting in lower release at pH 1.2. This behavior was similar to glutinous rice starch in formulation B2. In contrast, the drug release from films composed of chitosan and HPMC (formulation C2) showed little difference between pH 1.2 and 4.5. This is because HPMC is pH-independent, swelling to act as a barrier to sustain drug release and compensating for the low swelling ability of chitosan at pH 4.5, resulting in similar drug release profiles in both solutions.

To determine the drug release mechanism of EGCG from expandable films, the *in vitro* drug release data were fitted in various mathematical models: zero-order, first-order kinetics, Hixson–Crowell, Higuchi, and Korsmeyer–Peppas release models. The R^2 values for first-order kinetics were 0.996, 0.997, and 0.893 for formulations A2, B2, and C2, respectively, which were higher than those for zero-order kinetics in all three formulations. This indicates that EGCG release is concentration-dependent. Formulation A2 was fitted with the Hixson–Crowell model, which had the highest R^2 value (0.999), suggesting that EGCG release occurs primarily through dissolution, influenced by surface area and particle diameter. Formulation B2 followed first-order kinetics, confirming that EGCG concentration affects the release profile. Both the Hixson–Crowell and first-order kinetics results were further supported by Korsmeyer–Peppas models, where the release mechanism for formulations A2 and B2 was determined to be non-Fickian or anomalous diffusion, with n values of 0.8627 and 0.8710, respectively. This indicates a combination of diffusion and erosion mechanisms. On the other hand, formulation C2 fitted the Higuchi model ($R^2 = 0.934$), suggesting that diffusion is the primary release mechanism of this film.

Beyond drug release profiles, factors influencing EGCG solubility, stability, and absorption under gastrointestinal conditions (e.g., pH and enzymatic activity) should be explored to guide formulation strategies for improved gastric bioavailability and targeted delivery.

3.1.7. EGCG content determination

The actual EGCG content was found to be $97.97\% \pm 1.20\%$, $95.45\% \pm 2.19\%$, $92.71\% \pm 1.19\%$ of the theoretical loading for formulation A2, B2, C2, respectively. These values fall within the specified limits for content uniformity (85%–115%). Moreover, the uniformity of drug content in the formulations was confirmed by the low SD, which was less than 5.0%.

3.1.8. Morphology of the selected expandable film

The SEM images of formulation A2 are illustrated in Figure 4. The surface image of the composite films reveals no phase separation, indicating homogeneity. Additionally, the absence of polymer cracking suggests successful film formation after the drying process. The texture is relatively smooth, with slight roughness due to the high drug content in the polymers. The cross-section image shows polymer fibers within the film, with no visible cracking, confirming that the drying process led to the successful formation of films capable of carrying EGCG.

3.1.9. FTIR analysis

The EGCG spectrum displayed characteristic peaks at $1,692.1$ and $1,617.6$ cm^{-1} (C=O groups), $1,448.2$ cm^{-1} (C-H group), $1,346.5$ and $1,222.4$ cm^{-1} (O-C=O groups), $1,147.5$ and $1,097.0$ cm^{-1} (O-H groups), and $3,477.9$ and $3,357$ cm^{-1} (O-H groups) (Fig. 5). In the EGCG-loaded film, these functional groups were present, but the bands at $3,477.9$ and $3,357.1$ cm^{-1} merged into a broad band at $3,283.8$ cm^{-1} , indicating hydrogen bonding between the phenolic hydroxyl groups of EGCG and the O-H groups in the polymer matrix of the films.

3.1.10. X-ray diffraction studies

The X-ray diffractogram of EGCG (Fig. 6A) confirmed its crystalline morphology. In contrast, the diffractogram of the sample showed no characteristic peak corresponding to EGCG, indicating that EGCG was homogeneously dispersed in an amorphous state in the composite expandable films without altering the overall crystallinity of the film matrix. The amorphous form is known to possess higher free energy

and increased molecular mobility, which enhance dissolution rate and aqueous solubility. Therefore, formulating EGCG in an amorphous form may enhance bioavailability and support its therapeutic efficacy by improving absorption and systemic exposure.

3.1.11. Differential scanning calorimetry

The crystallinity of formulation A2 was confirmed by DSC, which is a crucial technique for analyzing the physicochemical interactions between the bioactive molecule and excipients in a formulation. DSC analysis (Fig. 6B) showed endothermic peaks for pure EGCG and the blank at 144.68°C and 135.29°C , respectively, corresponding to their melting points. Pure EGCG exhibited sharp peaks at 146.92°C , 193.25°C , and 244.83°C , indicating its crystalline nature. The sample displayed a broad peak at 144.25°C to 179.40°C , suggesting the melting point of EGCG combined with excipients. The DSC thermogram of the EGCG-excipient sample showed a reduced, shifted peak at 244.92°C , indicating solubilization of EGCG in the polymer matrix. These findings indicate reduced EGCG crystallinity and partial amorphization within the expandable drug delivery system, consistent with the X-ray diffraction (XRD) results.

3.1.12. In vitro biological activities of EGCG released from films

3.1.12.1. Determination of antioxidant activity

The results of the antioxidant activity assay are presented in Table 3. EGCG demonstrated potent antioxidant activity, with an IC_{50} value of 2.627 ± 0.166 $\mu\text{g}/\text{ml}$, attributed to its catechin or phenolic functional groups. Among the three expandable film formulations, A2, B2, and C2 exhibited IC_{50} values of 2.880 ± 0.116 , 2.814 ± 0.154 , and 2.676 ± 0.150 $\mu\text{g}/\text{ml}$, respectively. These values were comparable to that of the positive control, ascorbic acid, which had an IC_{50} value of 3.045 ± 0.117 $\mu\text{g}/\text{ml}$, indicating similar antioxidant potential. These results suggest that the films preserve the antioxidant activity of EGCG with minimal interference, and the hydrophilic nature of EGCG enhances its solubility and release from the film systems.

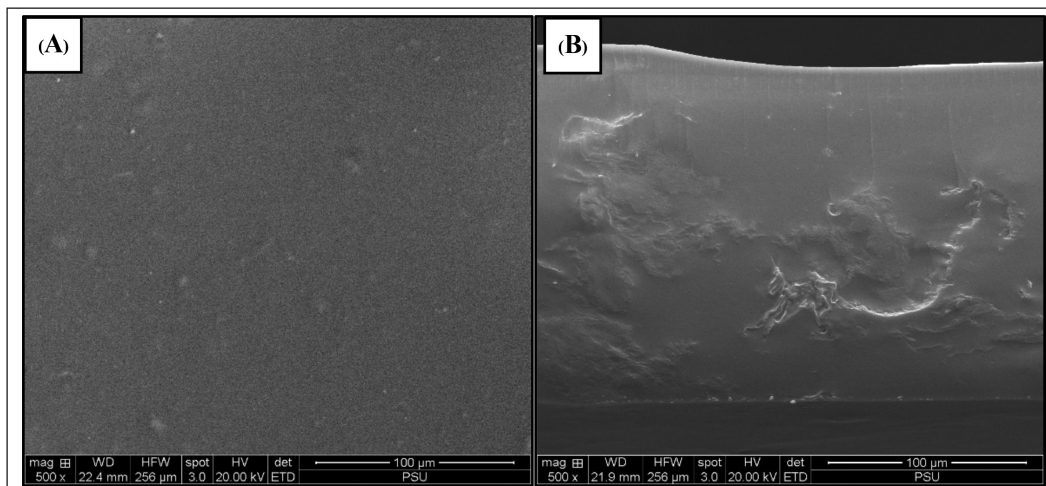


Figure 4. SEM images of (a) surface and (b) cross-section of EGCG-loaded films composed of konjac glucomannan and chitosan (formulation A2).

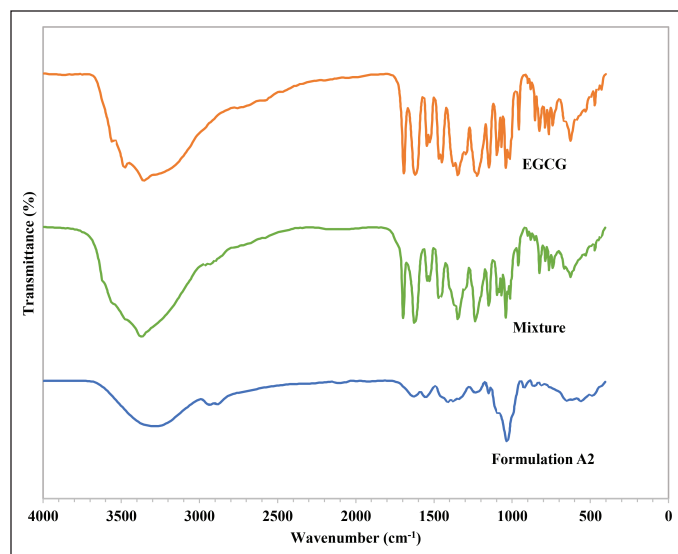


Figure 5. FTIR analysis of EGCG powder, mixture (EGCG, glucomannan, and chitosan), and expandable film (formulation A2).

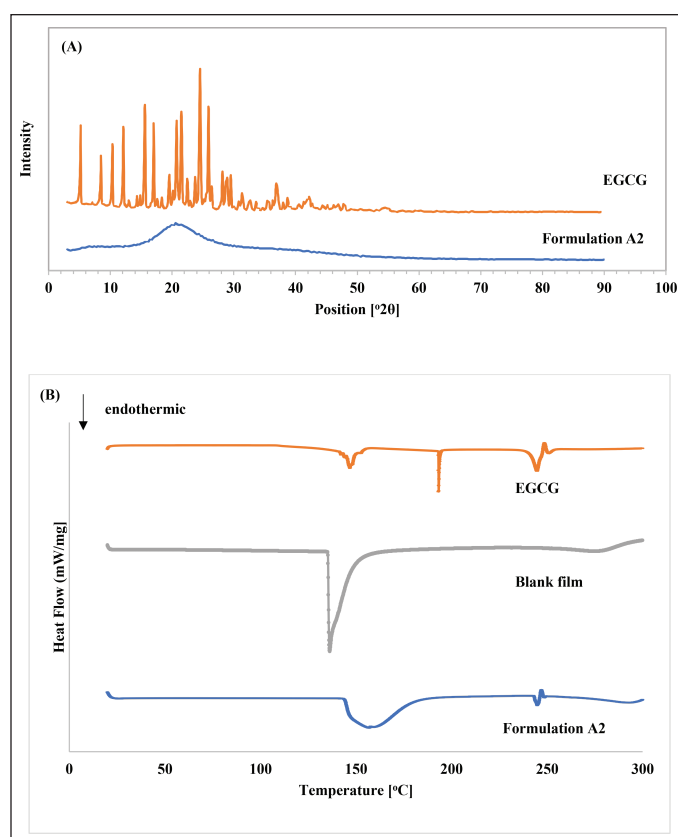


Figure 6. The XRD and DSC analysis of EGCG powder, and expandable film (formulation A2): (A) X-ray diffractogram; (B) DSC.

3.1.13. *In vitro* cytotoxic and anti-inflammatory activity

3.1.13.1. *In vitro* cytotoxicity test on macrophage cells

The cytotoxic activity was evaluated using the MTT assay to assess the effect of EGCG on murine macrophage cell lines (RAW 264.7). The cytotoxicity of EGCG standard

Table 3. Antioxidant activity of expandable film formulations containing EGCG.

Formulation	IC ₅₀ (ug/ml)
A2 (Konjac glucomannan)	2.880 ± 0.116
B2 (glutinous rice starch)	2.814 ± 0.154
C2 (HPMC)	2.676 ± 0.150
Ascorbic acid (positive control)	3.045 ± 0.117
EGCG powder (standard)	2.627 ± 0.166
Chitosan film without EGCG (negative control)	>100

All data are presented as $n = 3$, mean ± SD.

powder, formulation A2, blank A2, and indomethacin (positive control) was investigated 24-hour post-treatment. The MTT assay revealed that the highest dose of EGCG (100 µg/ml) in both the EGCG standard and formulation A2 reduced macrophage cell viability, although cell viability remained above 80% at all concentrations (100, 50, 25, 12.5, and 6.25 µg/ml), indicating no significant cytotoxicity. Based on these results, concentrations ranging from 6.25 to 100 µg/ml were selected for further investigations.

3.1.13.2. *Anti-inflammatory activity assay*

The anti-inflammatory effect of EGCG was assessed via NO inhibition in LPS-stimulated RAW 264.7 cells using the Griess assay (Fig. 7). In formulation A2, increasing EGCG concentrations (6.25, 12.5, 25, 50, and 100 µg/ml) resulted in dose-dependent NO reduction, with anti-inflammation activity percentages of 11.71% ± 1.75%, 29.69% ± 2.38%, 55.59% ± 1.45%, 74.20% ± 2.34%, and 88.05% ± 0.48 %, respectively, compared to LPS-treated controls. However, IC₅₀ of formulation A2 was 36.23 ± 0.93 µg/ml, slightly lower anti-inflammatory activity than that of EGCG powder (26.85 ± 0.49 µg/ml), possibly due to reduced EGCG stability in the chitosan-based formulation. Given this limitation, the stability of EGCG in the formulation should be further investigated. The anti-inflammatory activity of formulation A2 was comparable to indomethacin, used as a positive control (IC₅₀ of 32.72 ± 0.93 µg/ml). The blank A2 formulation also slightly inhibited NO inhibition, attributed to the inherent anti-inflammatory properties of chitosan [42]. EGCG-loaded chitosan-KGM films suppressed inducible nitric oxide synthase (iNOS) expression and NO production, consistent with the inflammatory pathway triggered by LPS-activated macrophages involving iNOS, TNF-α, IL-6, and IL-1β [43,44]. These findings align with other gastroretentive systems that reported comparable NO inhibition and cytokine suppression from chitosan-based superporous hydrogels containing resveratrol [45]. However, future studies are required to elucidate the specific molecular pathways by which the formulation exerts its anti-inflammatory effects.

Moreover, our results support the findings of Yuan *et al.* [46], where no significant difference in anti-inflammatory efficacy between EGCG alone and phosphatidylcholine-encapsulated EGCG in transdermal patches was observed. While phospholipid carriers enhance absorption, intrinsic activity of EGCG was not altered [46]. In contrast, our gastroretentive films offer both sustained gastric release and

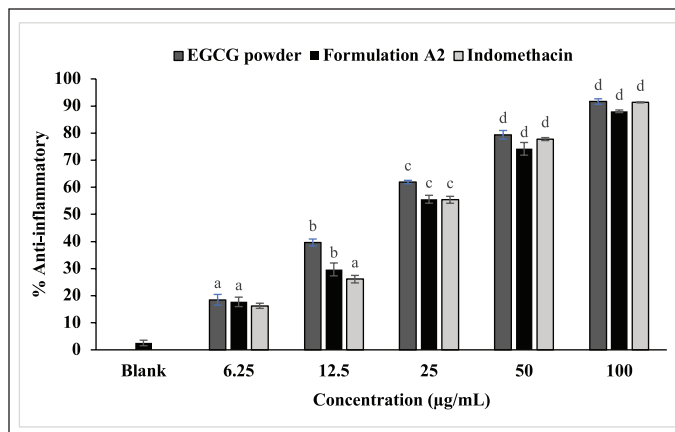


Figure 7. The anti-inflammatory effects were evaluated by measuring NO reduction in LPS-induced RAW 264.7 cells. Responses to various concentrations of EGCG standard powder and formulation A2 were compared with indomethacin ($n = 3$, mean \pm SD). Statistically significant differences were observed: ^acompared to blank formulation ($p < 0.05$); ^bcompared to the A2 formulation with 6.25 µg/ml EGCG ($p < 0.05$); ^ccompared to the A2 formulation with 12.5 µg/ml EGCG ($p < 0.05$); and ^dcompared to A2 formulation with 25 µg/ml EGCG ($p < 0.05$).

effective cytokine inhibition, presenting a promising strategy for localized treatment of gastrointestinal inflammation and improved oral bioavailability.

3.1.14. *In vitro* cytotoxic and anti-obesity activity

3.1.14.1. *In vitro* cytotoxicity test on adipose cells

Cytotoxicity of various concentrations (100, 50, 25, 12.5, and 6.25 µg/ml) of the formulation A2 and EGCG standard on 3T3-L1 adipose cells was investigated using the MTT assay. For formulations containing EGCG (A2), cell viability remained above 80% at concentration below 50 µg/ml, indicating non-cytotoxicity. On the other hand, adipocytes exposed to 100 µg/ml EGCG standard exhibited a cell viability of 56.6%, suggesting that EGCG concentrations above 100 µg/ml may induce cytotoxicity. Therefore, concentrations below 50 µg/ml were selected for subsequent experiments.

3.1.14.2. Anti-obesity activity

The anti-obesity potential of EGCG-loaded expanding gastro-retentive films was evaluated through their inhibitory effect on lipid accumulation in 3T3-L1 adipocytes. Differentiation of preadipocytes into mature adipocytes was confirmed by Oil Red O staining, with the negative control (undifferentiated, induction media), showing no lipid accumulation, and the positive control (differentiation media) exhibiting maximal lipid accumulation (100%).

Treatment with EGCG standard and expandable film sample (formulation A2) suppressed lipid accumulation with increasing EGCG concentrations of 2, 10, and 50 µg/ml. At 50 µg/ml, both treatments reduced lipid accumulation by approximately 30%, with formulation A2 yielding $65.53\% \pm 4.26\%$ lipid content relative to the control (Fig. 8). This effect was comparable to the EGCG standard, demonstrating the preserved bioactivity of EGCG upon release from the film matrix. These findings are consistent with published report that EGCG downregulated key

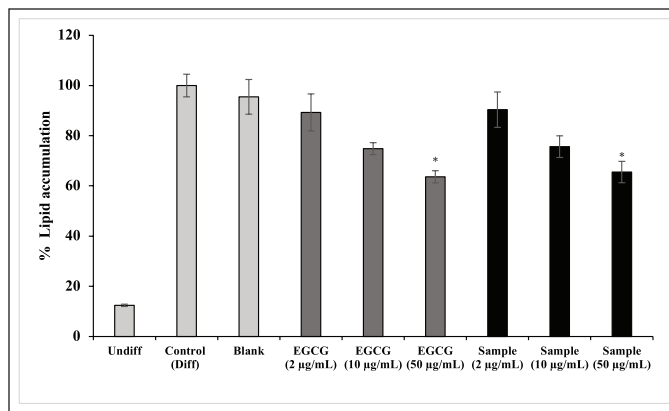


Figure 8. 3T3-L1 adipocytes were treated with blank, undifferentiated control, differentiated control, EGCG standard powder, and formulation A2 sample (2, 10, 50 µg/ml) to induce differentiation. Differentiation was quantified by absorbance at 570 nm, with control cells set to 100%. Data are represented as mean \pm SD ($n = 3$). * $p < 0.05$ compared with differentiated control.

adipogenic regulators-PPAR γ and PPAR α -during differentiation [47]. Additionally, a dose-dependent reduction in lipid droplet formation was observed, accompanied by lower levels of adipokines (adiponectin and leptin) and lipogenic enzymes such as fatty acid synthase, reinforcing EGCG's role in suppressing adipogenesis through multiple pathways, including inhibition of glucose uptake and lipid accumulation [48].

The gastroretentive film system developed in this study offers several advantages over conventional EGCG delivery routes. Sustained release within the stomach not only improves the stability and local concentration of EGCG but also enhances its bioavailability, potentially leading to greater systemic metabolic effects. This is particularly relevant for targeting the early stages of fat metabolism in the digestive tract. Compared to other systems, such as the *in situ* gelling formulation of *Garcinia* extract, which inhibited lipid accumulation by ~35% but showed cytotoxicity at higher doses, our formulation demonstrated comparable efficacy without cytotoxic effects at the tested concentrations [49]. Together, these results highlight the promising anti-obesity activity of EGCG when delivered via chitosan-KGM expanding films, providing a safe, effective, and targeted strategy for obesity management through gastric retention and controlled release.

4. CONCLUSION

Novel expandable gastro-retentive dosage forms were developed to deliver EGCG, a natural compound with antioxidant, anti-inflammatory, and anti-obesity properties, using various hydrophilic polymers. A composite film based on chitosan, combined with 1.0% KGM as an additional film-forming agent (formulation A2), incorporating 100 mg of EGCG per individual film unit and supplemented with SA and glycerin to enhance gelling strength and elasticity, respectively, demonstrated optimal physicochemical characteristics. It exhibited high swelling capacity, significant expansion, and sustained EGCG release of over 80% within 8 hours. Additionally, it possessed sufficient mechanical strength to withstand gastric forces. Bioactivity studies confirmed its antioxidant and anti-inflammatory effects in RAW 264.7 macrophage cells, comparable to indomethacin, as well as anti-obesity activity in 3T3-L1 adipose cells. These

findings highlight the potential of expandable gastro-retentive formulations for the effective delivery of EGCG in anti-inflammatory and anti-obesity applications. Future research should focus on *in vivo* studies to verify gastro-retentive behavior, pharmacokinetics, and therapeutic efficacy. Additionally, long-term stability, safety, and scale-up feasibility should be investigated to improve clinical outcomes.

5. ACKNOWLEDGMENTS

The authors would like to acknowledge financial support from the Project of Strengthening Excellence in Pharmacy, Faculty of Pharmaceutical Sciences, Prince of Songkla University.

6. AUTHOR CONTRIBUTIONS

All authors made substantial contributions to conception and design, acquisition of data, or analysis and interpretation of data; took part in drafting the article or revising it critically for important intellectual content; agreed to submit to the current journal; gave final approval of the version to be published; and agree to be accountable for all aspects of the work. All the authors are eligible to be an author as per the International Committee of Medical Journal Editors (ICMJE) requirements/guidelines.

7. CONFLICTS OF INTEREST

The authors report no financial or any other conflicts of interest in this work.

8. ETHICAL APPROVALS

This study does not involve experiments on animals or human subjects.

9. DATA AVAILABILITY

All data generated and results were included in this research article.

10. PUBLISHER'S NOTE

All claims expressed in this article are solely those of the authors and do not necessarily represent those of the publisher, the editors and the reviewers. This journal remains neutral with regard to jurisdictional claims in published institutional affiliation.

11. USE OF ARTIFICIAL INTELLIGENCE (AI)-ASSISTED TECHNOLOGY

The authors declare that they have not used artificial intelligence (AI)-tools for writing and editing of the manuscript, and no images were manipulated using AI.

REFERENCES

1. Yang CS, Gang C, Qing W. Recent scientific studies of a traditional Chinese medicine, tea, on prevention of chronic disease. *J Tradit Complement Med.* 2014;4(1):17–23. doi: <http://doi.org/10.4103/2225-4110.12436>
2. Chacko SM, Thambi PT, Kuttan R, Nishigaki I. Beneficial effects of green tea: a literature review. *Chin Med.* 2010;5:13. doi: <https://doi.org/10.1186/1749-8546-5-13>
3. Baek N, Kim Y, Duncan S, Leitch K, O'Keefe S. (-)-Epigallocatechin gallate stability in ready-to-drink (RTD) green tea infusions in TiO₂ and oleic-acid-modified TiO₂ polylactic acid film packaging stored under fluorescent light during refrigerated storage at 4 °C. *Foods* 2021;10:723. doi: <http://doi.org/10.3390/foods10040723>
4. Kim HS, Quon MJ, Kim JA. New Insights into the mechanisms of polyphenols beyond antioxidant properties; lessons from the green tea polyphenol, epigallocatechin 3-gallate. *Redox Biol.* 2014;2:187–95. doi: <http://doi.org/10.1016/j.redox.2013.12.022>
5. Casanova E, Salvado J, Crescenti A, Gibert-Ramos A. Epigallocatechin gallate modulates muscle homeostasis in type 2 diabetes and obesity by targeting energetic and redox pathways: a narrative review. *Int J Mol Sci.* 2019;20(3):532. doi: <http://doi.org/10.3390/ijms20030532>
6. Hayashi A, Terasaka S, Nukada Y, Kameyama A, Yamane M, Shioi R, *et al.* 4-Sulfation is the major metabolic pathway of epigallocatechin-3-gallate in human: characterization of metabolites, enzymatic analysis, and pharmacokinetic profiling. *J Agric Food Chem.* 2022;70(27):8264–73. doi: <http://doi.org/10.1021/acs.jafc.2c02150>
7. Vinchurkar K, Sainy J, Khan MA, Mane S, Mishra DK, Dixit P. Features and facts of a gastroretentive drug delivery system – a review. *Turk J Pharm Sci.* 2022;19(4):476–87. doi: <http://doi.org/10.4274/tips.galenos.2021.44959>
8. Tripathi J, Thapa P, Maharjan R, Jeong SH. Current state and future perspectives on gastroretentive drug delivery systems. *Pharmaceutics* 2019;11(4):193. doi: <http://doi.org/10.3390/pharmaceutics11040193>
9. Ohki T, Ni Q, Ohsako N, Iwamoto M. Mechanical and shape memory behavior of composites with shape memory polymer. *Compos Part A Appl Sci Manuf.* 2004;35(9):1065–73. doi: <http://doi.org/10.1016/j.compositesa.2004.03.001>
10. Klausner EA, Lavy E, Friedman M, Hoffman A. Expandable gastroretentive dosage forms. *J Control Release.* 2003;90(2):143–62. doi: [https://doi.org/10.1016/S0168-3659\(03\)00203-7](https://doi.org/10.1016/S0168-3659(03)00203-7)
11. Vassiliadi E, Aridas A, Schmitt V, Xenakis A, Zoumpantioti M. (Hydroxypropyl)methylcellulose-chitosan film as a matrix for lipase immobilization: operational and morphology study. *J Mol Catal.* 2022;522:112252. doi: <http://doi.org/10.1016/j.mcat.2022.112252>
12. Saberian M, Roudsari RS, Haghshenas N, Rousta A, Alizadeh S. How the combination of alginate and chitosan can fabricate a hydrogel with favorable properties for wound healing. *Heliyon* 2024;10(11):e32040. doi: <https://doi.org/10.1016/j.heliyon.2024.e32040>
13. Li C, Shang W, Huang Y, Ge J, Ye J, Xin Qu X, *et al.* Sodium alginate/chitosan composite scaffold reinforced with biodegradable polyesters/gelatin nanofibers for cartilage tissue engineering. *Int J Biol Macromol.* 2025;285:138054. doi: <https://doi.org/10.1016/j.ijbiomac.2024.138054>
14. Shuzhen N, Liang J, Hui Z, Yongchao Z, Guigan F, Huining X. Enhancing hydrophobicity, strength and UV shielding capacity of starch film via novel co-cross-linking in neutral conditions. *R Soc Open Sci.* 2018;5(11):181206. doi: <http://doi.org/10.1098/rsos.181206>
15. Alonso-Sande M, Teijeiro-Osorio D, Remunan-Lopez C, Alonso MJ. Glucomannan, A Promising polysaccharide for biopharmaceutical purposes. *Eur J Pharm Biopharm.* 2009;72:453–46. doi: <https://doi.org/10.1016/j.ejpb.2008.02.005>
16. Zhang C, Chen JD, Yang FQ. Konjac glucomannan, a promising polysaccharide for OCDDS. *Carbohydr Polym.* 2014;104:175–81. doi: <https://doi.org/10.1016/j.carbpol.2013.12.081>
17. Ni Y, Liu Y, Zhang W, Shi S, Zhu W, Wang R, *et al.* Advanced honjac glucomannan-based films in food packaging: classification, preparation, formulation mechanism and function. *LWT-Food Sci Technol.* 2021;152:112338. doi: <https://doi.org/10.1016/j.lwt.2021.112338>
18. Chen J, Li X, Chen L, Xie F. Starch film-coated microparticles for oral colon-specific drug delivery. *Carbohydr Polym.* 2018;191:242–54. doi: <https://doi.org/10.1016/j.carbpol.2018.03.025>
19. Thakur R, Pristijono P, Scarlett CJ, Bowyer M, Singh SP, Vuong QV. Starch-based films: major factors affecting their properties. *Int J Biol Macromol.* 2019;132:1079–89. doi: <https://doi.org/10.1016/j.ijbiomac.2019.03.190>

20. Akinosho H, Hawkins S, Wicker L. Hydroxypropyl methylcellulose substituent analysis and rheological properties. *Carbohydr Polym.* 2013;98(1):276–81. doi: <https://doi.org/10.1016/j.carbpol.2013.05.081>
21. Gökmen FÖ, Bayramgil NP. Preparation and characterization of some cellulose derivatives nanocomposite films. *Carbohydr Polym.* 2022;297:120030. doi: <https://doi.org/10.1016/j.carbpol.2022.120030>
22. Laracuate ML, Yu MH, McHugh KJ. Zero-order drug delivery: state of the art and future prospects. *J Contr Release.* 2020;327:834–56. doi: <https://doi.org/10.1016/j.jconrel.2020.09.020>
23. Behera SS, Ray RC. Konjac glucomannan, a promising polysaccharide of *Amorphophallus konjac* K. koch in health care. *Int J Biol Macromol.* 2016;92:942–56. doi: <https://doi.org/10.1016/j.ijbiomac.2016.07.098>
24. Jahromi LP, Ghazali M, Ashrafi H, Azadi A. A comparison of models for the analysis of the kinetics of drug release from PLGA-based nanoparticles. *Heliyon* 2020;6(2):e03451. doi: <https://doi.org/10.1016/j.heliyon.2020.e03451>
25. Paul DR. Elaborations on the Higuchi model for drug delivery. *Int J Pharm.* 2011;418(1):13–7. doi: <https://doi.org/10.1016/j.ijpharm.2010.10.037>
26. Zhu W, Long J, Shi M. Release kinetics model fitting of drugs with different structures from viscose fabric. *Materials* 2023;16(8):3282. doi: <https://doi.org/10.3390/ma16083282>
27. Singh M, Lee KE, Vinayagam R, Kang SG. Antioxidant and antibacterial profiling of pomegranate-pericarp extract functionalized-zinc oxide nanocomposite. *Biotechnol Bioprocess Eng.* 2021;26:728–37. doi: <http://doi.org/10.1007/s12257-021-02111-1>
28. Siriprukpong W, Praparatana R, Issarachot O, Wiwattanapatapee R. Simultaneous delivery of curcumin and resveratrol via *in situ* gelling, raft-forming, gastroretentive formulations. *Pharmaceutics* 2024;16:641. doi: <http://doi.org/10.3390/pharmaceutics16050641>
29. Chen J, Liu C, Chen Y, Chen Y, Chang PR. Structural characterization and properties of starch/konjac glucomannan blend films. *Carbohydr Polym.* 2008;74(4):946–52. doi: <http://doi.org/10.1016/j.carbpol.2008.05.021>
30. Kaewkroek K, Petchsomrit A, Septama AW, Wiwattanapatapee R. Development of starch/chitosan expandable films as a gastroretentive carrier for ginger extract-loaded solid dispersion. *Saudi Pharm J.* 2022;30(2):120–31. doi: <http://doi.org/10.1016/j.jsps.2021.12.017>
31. Xu YX, Kim KM, Hanna MA, Nag D. Chitosan–starch composite film: preparation and characterization. *Ind Crop Prod.* 2005;21(2):185–92. doi: <https://doi.org/10.1016/j.indcrop.2004.03.002>
32. Soe MT, Pongjanyakul T, Limpongsa E, Jaipakdee N. Modified glutinous rice starch-chitosan composite films for buccal delivery of hydrophilic drug. *Carbohydr Polym.* 2020;245:116556. doi: <http://doi.org/10.1016/j.carbpol.2020.116556>
33. Kraisit P, Limmatvapirat S, Nunthanid J, Sriamornsak P, Luangtana-Anan M. Preparation and characterization of hydroxypropyl methylcellulose/polycarbophil mucoadhesive blend films using a mixture design approach. *Chem Pharm Bull.* 2017;65(3):284–94. doi: <https://doi.org/10.1248/cpb.c16-00849>
34. Zanchetta FC, De Wever P, Morari J, Gaspar RC, Prado TP, De Maeseneer T, *et al.* *In vitro* and *in vivo* evaluation of chitosan/HPMC/insulin hydrogel for wound healing applications. *Bioengineering* 2024;11(2):168. doi: <https://doi.org/10.3390/bioengineering11020168>
35. Li S, Lyu H, Wang Y, Kong X, Wu X, Zhang L, *et al.* Two-way reversible shape memory behavior of chitosan/glycerol film triggered by water. *Polymer* 2023;15:2380. doi: <http://doi.org/10.3390/polym15102380>
36. Ma S, Zheng Y, Zhou R, Ma M. Characterization of chitosan films incorporated with different substance of konjac glucomannan, cassava starch, maltodextrin and gelatin, and application in mongolian cheese packaging. *Coatings* 2021;11:88. doi: <http://doi.org/10.3390/coatings11010084>
37. Boontawee R, Issarachot O, Kaewkroek K, Wiwattanapatapee R. Foldable/expandable gastro-retentive films based on starch and chitosan as a carrier for prolonged release of resveratrol. *Curr Pharm Biotechnol.* 2022;23(7):1009–18. doi: <http://doi.org/10.2174/1389201022666210615115553>
38. Llanes L, Dubessay P, Pierre G, Delattre C, Michaud P. Biosourced polysaccharide-based superabsorbents. *Polysaccharides* 2020;1(1):51–79. doi: <https://doi.org/10.3390/polysaccharides1010005>
39. Sivanewari S, Karthikeyan E, Chandana PJ. Novel expandable gastro retentive system by unfolding mechanism of levetiracetam using simple lattice design – formulation optimization and *in vitro* evaluation. *Bull Fac Pharm Cairo Univ.* 2017;55(1):63–72. doi: <http://doi.org/10.1016/j.bfopcu.2017.02.003>
40. Basak S, Singhal RS. Inclusion of konjac glucomannan in pea protein hydrogels improved the rheological and *in vitro* release properties of the composite hydrogels. *Int J Biol Macromol.* 2024;257(2):128689. doi: <https://doi.org/10.1016/j.ijbiomac.2023.128689>
41. Alvarez-Manceñido F, Landin M, Lacik I, Martínez-Pacheco R. Konjac glucomannan and konjac glucomannan/xanthan gum mixtures as excipients for controlled drug delivery systems. Diffusion of small drugs. *Int J Pharm.* 2008;349(1–2):11–8. doi: <http://doi.org/10.1016/j.ijpharm.2007.07.015>
42. Chang SH, Lin YY, Wu GJ, Huang CH, Tsai GJ. Effect of chitosan molecular weight on anti-inflammatory activity in the RAW 264.7 macrophage model. *Int J Biol Macromol.* 2019;131:167–75. doi: <https://doi.org/10.1016/j.ijbiomac.2019.02.066>
43. Hossen I, Kaiqi Z, Hua W, Junsong X, Mingquan H, Yanping C. Epigallocatechin gallate (EGCG) inhibits lipopolysaccharide-induced inflammation in RAW 264.7 macrophage cells via modulating nuclear factor kappa-light-chain enhancer of activated B cells (NF- κ B) signaling pathway. *Food Sci Nutr.* 2023;11(8):4634–50. doi: <https://doi.org/10.1002/fsn3.3427>
44. Sun W, Yu Z, Yang S, Jiang C, Kou Y, Xiao L, *et al.* A transcriptomic analysis reveals novel patterns of gene expression during 3T3-L1 adipocyte differentiation. *Front Mol Biosci.* 2020;7:564339. doi: <http://doi.org/10.3389/fmolb.2020.564339>
45. Issarachot O, Bunlung S, Kaewkroek K, Wiwattanapatapee R. Superporous hydrogels based on blends of chitosan and polyvinyl alcohol as a carrier for enhanced gastric delivery of resveratrol. *Saudi Pharm J.* 2023;31(3):335–47. doi: <http://doi.org/10.1016/j.jsps.2023.01.001>
46. Yuan M, Hu L, Zhu C, Li Q, Tie H, Ruan H, *et al.* Comparison and assessment of anti-inflammatory and antioxidant capacity between EGCG and phosphatidylcholine-encapsulated EGCG. *J Cosmet Dermatol.* 2025;24(1):e16628. doi: <http://doi.org/10.1111/jocd.16628>
47. Wang Y, Li C, Peng W, Sheng J, Zi C, Wu X. EGCG suppresses adipogenesis and promotes browning of 3T3-L1 cells by inhibiting notch1 expression. *Molecules* 2024;29(11):2555. doi: <http://doi.org/10.3390/molecules29112555>
48. Lu Y, Chen J, Xian T, Zhou Y, Yuan W, Wang M, *et al.* Epigallocatechin-3-gallate suppresses differentiation of adipocytes via regulating the phosphorylation of FOXO1 mediated by PI3K-AKT signaling in 3T3-L1 cells. *Oncotarget* 2017;9(7):7411–23. doi: <http://doi.org/10.18632/oncotarget.23590>
49. Fungfoung K, Praparatana R, Issarachot O, Wiwattanapatapee R. Development of oral *in situ* gelling liquid formulations of garcinia extract for treating obesity. *Gels* 2023;9:660. doi: <http://doi.org/10.3390/gels9080660>

How to cite this article:

Lakhiew A, Praparatana R, Sangsen Y, Wiwattanapatapee R. Enhanced oral delivery of epigallocatechin gallate via expanding gastro-retentive films composed of chitosan and konjac glucomannan blends. *J Appl Pharm Sci.* 2026;16(01):095-108. DOI: 10.7324/JAPS.2025.251914